INVITED PAPER *Special Section on Cutting-Edge Technologies of Superconducting Electronics*

Improved Liquid-Phase Detection of Biological Targets Based on Magnetic Markers and High-Critical-Temperature Superconducting Quantum Interference Device

Masakazu URA[†], **Kohei NOGUCHI**[†], **Yuta UEOKA**[†], **Kota NAKAMURA**[†], ***Nonmembers***, **Teruyoshi SASAYAMA**[†], ***Member***, **Takashi YOSHIDA**[†], ***Nonmember***, ***and*** **Keiji ENPUKU**[†a)], ***Member***

SUMMARY In this paper, we propose improved methods of liquid-phase detection of biological targets utilizing magnetic markers and a high-critical-temperature superconducting quantum interference device (SQUID). For liquid-phase detection, the bound and unbound (free) markers are magnetically distinguished by using Brownian relaxation of free markers. Although a signal from the free markers is zero in an ideal case, it exists in a real sample on account of the aggregation and precipitation of free markers. This signal is called a blank signal, and it degrades the sensitivity of target detection. To solve this problem, we propose improved detection methods. First, we introduce a reaction field, B_{re}, during the binding reaction between the markers and targets. We additionally introduce a dispersion process after magnetization of the bound markers. Using these methods, we can obtain a strong signal from the bound markers without increasing the aggregation of the free markers. Next, we introduce a field-reversal method in the measurement procedure to differentiate the signal from the markers in suspension from that of the precipitated markers. Using this procedure, we can eliminate the signal from the precipitated markers. Then, we detect biotin molecules by using these methods. In an experiment, the biotins were immobilized on the surfaces of large polymer beads with diameters of 3.3 μm. They were detected with streptavidin-conjugated magnetic markers. The minimum detectable molecular number concentration was 1.8×10^{-19} mol/ml, which indicates the high sensitivity of the proposed method.

key words: *high-critical-temperature superconducting quantum interference device (SQUID), magnetic marker, immunoassays, liquid-phase detection*

1. Introduction

Magnetic immunoassay techniques that utilize Brownian relaxation of magnetic markers have been developed for liquid-phase detection of biological targets [1]–[16]. In techniques of this type, the bound and free markers are magnetically distinguished using the Brownian relaxation of the markers. To date, several detection methods, including AC susceptibility [1]–[6], magnetic relaxation [7]–[13], and remanence measurement [14]–[16], have been developed. These methods eliminate the need for a time-consuming washing process for marker separation.

We have therefore developed a liquid-phase detection technique that employs large polymer beads that immobilize the bound markers [14]–[16]. In this method, biological targets are fixed on the surface of large polymer beads with sizes typically on the order of μm. In this case, the Brownian relaxation time of the bound marker becomes much longer than that of the free markers. Namely, the signal from the bound markers is retained for a long time period on account of the long relaxation times of the markers. On the other hand, the signal from the free markers rapidly decays to zero on account of their short relaxation times. As a result, the bound and free markers can be magnetically distinguished.

The signal from the free markers is zero in an ideal case; however, in a practical sample, the signal is present. In the practical sample, two types of markers exist in addition to the bound and free markers. One is the agglomerate of free markers. The other is comprised of the markers that are precipitated or absorbed on the bottom of the reaction well. Because the Brownian relaxation of these markers is deteriorated, the signal is generated from these markers [16]. This signal is called a blank signal, and it degrades the target detection performance. Therefore, it is necessary to solve this problem to further improve the detection sensitivity.

In this paper, we propose methods that can decrease the blank signal from the free markers. First, we present improved methods for sample preparation and magnetization of the bound markers. We introduce a reaction field, $B_{re} = 1.5$ mT, during the binding reaction between the markers and targets. We additionally introduce a dispersion process after magnetization of the bound markers. Next, we propose a measurement procedure to distinguish the signal from the markers in suspension from that of the precipitated markers. Using these methods, we can obtain a strong signal from the bound markers without increasing the blank signal of the free markers. Finally, we demonstrate the detection of biotin molecules. The minimum detectable molecular number concentration is 1.8×10^{-19} mol/ml, which indicates the high sensitivity of the proposed method.

2. Principle of Liquid-Phase Detection

Figure 1 (a) schematically depicts the measurement system for liquid-phase target detection. As shown in Fig. 1 (b), biological targets are fixed to large polymer beads with diameters of $d_p = 3.3$ μm. The magnetic markers are bound to the targets for detection. The bound and free markers coexist in the sample solution. The hydrodynamic diameter of the marker is $d_h = 200$ nm. The Brownian relaxation times of

Manuscript received October 23, 2015.
Manuscript revised December 24, 2015.
[†]The authors are with the Department of Electrical Engineering, Kyushu University, Fukuoka-shi, 819–0395 Japan.
a) E-mail: enpuku@sc.kyushu-u.ac.jp
DOI: 10.1587/transele.E99.C.669

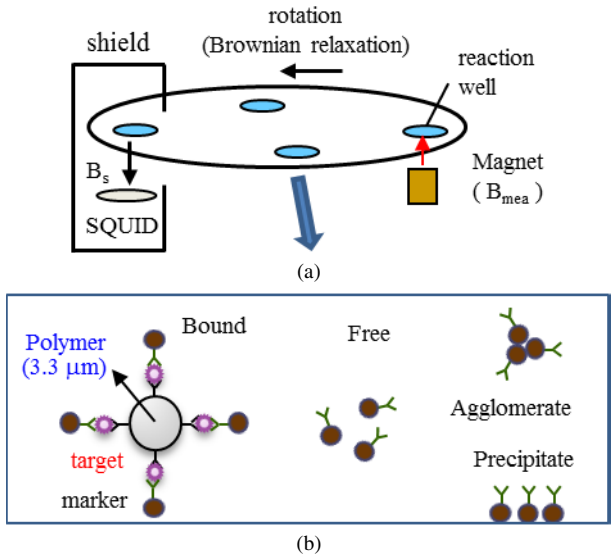

Fig. 1 (a) Schematic diagram of the detection system, and (b) markers in the practical sample.

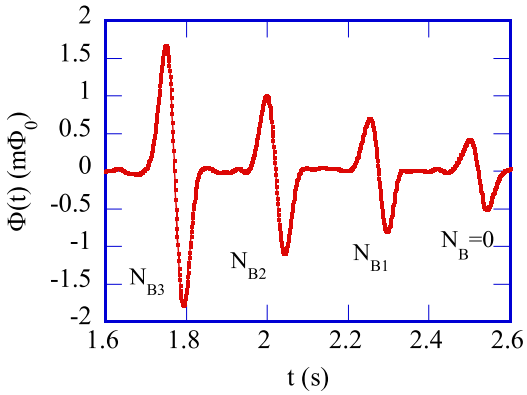

Fig. 2 Waveform of the signals from the four reaction wells with different concentrations of the targets (biotin molecules). The number of biotins is $N_{B1} = 2 \times 10^4$, $N_{B2} = 5 \times 10^4$, and $N_{B3} = 10^5$. The measurement field was $B_{mea} = 1$ mT.

the free and bound markers are calculated using the relation $\tau_B = (\pi\eta/2k_BT)d^3$, where $\eta = 1 \times 10^{-3}$ Pa·s is the viscosity of water, k_B is the Boltzmann constant, $T = 300$ K, and d is the diameter of the particle. Using the values of d_h and d_p for d, they are determined to be $\tau_B = 6$ ms and 13 s for the free and bound markers, respectively.

The sample solution, including both the bound and free markers, is placed in a reaction well, as shown in Fig. 1 (a). The bound and free markers are magnetically distinguished by the difference between their Brownian relaxation times. Details of this detection principle have been described elsewhere [16]. Briefly, a measurement field, $B_{mea} = 1$ mT, is applied to measure the magnetic (remanence) signals from the bound markers, as shown in Fig. 1 (a). When the sample plate is rotated and the reaction well is free from the magnetic field of the magnet, so that $B = 0$, the free markers undergo Brownian relaxation. After $T = 1.5$ s, the reaction well is brought above the superconducting quantum interference device (SQUID). In that position, the signal from the free markers decays to zero; therefore, only the signal from the bound markers is detectable.

In our study, the signal from the markers is detected with a high-critical-temperature SQUID, which includes a ramp-edge Josephson junction [17]. The flux noise at 77 K is $S_\Phi^{1/2} = 7.5\ \mu\Phi_0/\mathrm{Hz}^{1/2}$ in the white noise region, and 14 $\mu\Phi_0/\mathrm{Hz}^{1/2}$ at $f = 1$ Hz when SQUID is operated in the AC bias mode.

The sample plate has twelve reaction wells. By rotating the sample plate, we can measure the signal from each reaction well. Figure 2 depicts the waveform of the signals, $\Phi(t)$, which were obtained from the four reaction wells with different concentrations of the targets (biotin molecules). As shown, the amplitude of the signal increases with the increase of the number of targets, N_B. The peak-to-peak value of the signal is defined as the signal, Φ_s, from the markers in each sample.

As shown in Fig. 2, the blank signal is obtained even in the absence of the target (i.e., for the case of $N_B = 0$). However, as noted above, it should be zero in the ideal case. As depicted in Fig. 1 (b), the two types of markers—the agglomerate of free markers and those precipitated or absorbed on the bottom of the reaction well—exist in addition to the bound and free markers in the practical sample. As mentioned, the Brownian relaxation of these markers is deteriorated; accordingly, the blank signal is generated from these markers [16].

This blank signal affects the sensitivity of target detection. To perform highly sensitive detection, the ratio between the signal from the bound markers and the blank signal must be increased. In the following section, we demonstrate the improvement in the detection procedure for this purpose.

3. Sample Preparation and Magnetization

In the experiment, we used biotin molecules as targets. Approximately 1,300 biotins were conjugated to a single polymer bead. Streptavidin-conjugated magnetic markers (FG beads, Tamagawa Seiki) were put in the sample solution for detection. These markers were bound to the biotins, as illustrated in Fig. 1 (b). The binding reaction was performed for 60 min at 30 °C in a phosphate buffer solution. For detection, 60 μL of the sample was deposited into a well, as shown in Fig. 1 (a). Concentration of the number of biotin-conjugated polymer beads was changed from 5 to 100/60 μL in order to detect biotin molecules from 6.5×10^3 to 1.3×10^5/60 μL. Concentration of the magnetic markers was 1 μg/60 μL. It should be noted that the Néel relaxation time of the present marker is very long, and the marker generates the remanence signal after magnetization [16].

We studied four different methods for sample preparation and magnetization, as listed on Table 1.

- In method A, the sample is prepared using a conventional technique.

Table 1 Four procedures for sample preparation and magnetization

Method	Reaction field B_{re}	Magnetization B_{mag}	Dispersion process
A	—	—	—
B	○	—	—
C	○	○	—
D	○	○	○

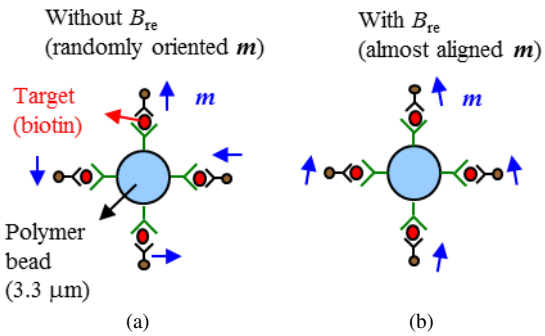

Fig. 3 Magnetic moment $\boldsymbol{m}$ of the bound markers at the end of the binding reaction. (a) $\boldsymbol{m}$ is randomly oriented without B_{re}. (b) $\boldsymbol{m}$ is almost aligned when B_{re} is applied.

- In method B, the sample is prepared using a reaction field, B_{re} = 1.5 mT.
- In method C, the sample is magnetized after applying method B by using a magnetization field of B_{mag} = 40 mT.
- In method D, the dispersion process using a vortex stirring is performed after method C.

3.1 Binding Reaction Using Reaction Field B_{re}

First, we compared method A with method B, as listed in Table 1. Method A is a conventional sample preparation technique. Using method B, we introduced a weak magnetic field during the binding reaction between the targets and markers. This field was denoted by the reaction field, B_{re} [18]. In Fig. 3, the effect of B_{re} is schematically presented. In the absence of B_{re}, the markers rotate in the solution during the binding reaction on account of the Brownian rotation. As a result, the magnetic moment, $\boldsymbol{m}$, of the bound markers was randomly oriented when the binding reaction was finished, as shown in Fig. 3 (a). However, when field B_{re} was applied, the moments of the markers were aligned to the direction of B_{re} during the reaction. Hence, the markers were bound to the targets with their moments $\boldsymbol{m}$ almost aligned, as shown in Fig. 3 (b). This contrasted with the conventional case without B_{re}. Owing to the alignment of the moments $\boldsymbol{m}$, the bound markers could be easily magnetized.

To determine the strength of field B_{re}, we measured the magnetization curve of the markers in the solution. In Fig. 4, the measured magnetic moment of the sample, $\langle m \rangle$, is shown by circles when the weak field, H, is applied. It is well known that the value of the magnetic moment of the

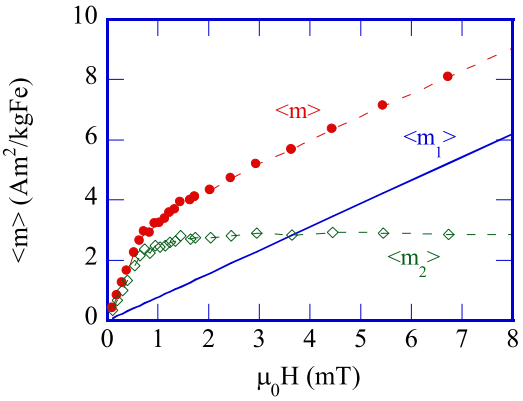

Fig. 4 Low field magnetization curve of the markers in solution. Experimental value $\langle m \rangle$ can be divided into two terms, $\langle m \rangle = \langle m_1 \rangle + \langle m_2 \rangle$.

marker, m, is distributed in the sample [19]. It is also shown that, for the markers that show remanence after magnetization, the distribution can be approximated by using two typical values of m [20]. Hence, we assume that $\langle m \rangle$ can be expressed by the sum of two terms, $\langle m \rangle = \langle m_1 \rangle + \langle m_2 \rangle$. Here, $\langle m_1 \rangle$ is given by the markers with small m values, and it linearly increases with H. On the other hand, $\langle m_2 \rangle$ is given by the markers with large m values, whose behaviors in solution are given by the Langevin function $L(\xi) = \coth(\xi) - 1/\xi$ with $\xi = \mu_0 Hm/k_B T$.

In Fig. 4, we show the $\langle m_1 \rangle$-H and $\langle m_2 \rangle$-H curves. $\langle m_1 \rangle$ is obtained from the linear part of the $\langle m \rangle$-H curve at high values of H, whereas $\langle m_2 \rangle$ is obtained by subtracting $\langle m_1 \rangle$ from $\langle m \rangle$. When we fit the $\langle m_2 \rangle$-H curve with the Langevin function, we get $m = 2 \times 10^{-17}$ Am^2.

As shown in Fig. 4, $\langle m_2 \rangle$ is saturated for the field values greater than 1.5 mT. This means that markers with large m values are aligned in the solution by field H. Therefore, we selected reaction field B_{re} = 1.5 mT in the following experiment: We applied B_{re} = 1.5 mT for 60 min during the binding reaction between the targets and markers.

In Fig. 5 (a), the blank and bound signals obtained for methods A and B are shown. The blank signal indicates the signal from the free markers in the absence of targets, specifically when the number of biotin molecules is $N_B = 0$. The bound signal indicates the signal from the markers that are bound to the targets when $N_B = 1.3 \times 10^5$. By comparing the results of cases A and B, the effect of reaction field B_{re} is evident.

As shown in Fig. 5 (a), the blank signal is almost the same for the A (B_{re} = 0) and B (B_{re} = 1.5 mT) cases. This result reveals that the aggregation of the free markers due to reaction field B_{re} is very small. However, a larger bound signal is obtained for case B. The bound signal is increased by approximately five times compared to case A. This is because the markers are bound to the targets with their moments $\boldsymbol{m}$ almost aligned when the reaction field of B_{re} = 1.5 mT is used, as shown in Fig. 3 (b).

In Fig. 5 (b), the ratio between the bound and blank signals defined by the following equation is shown.

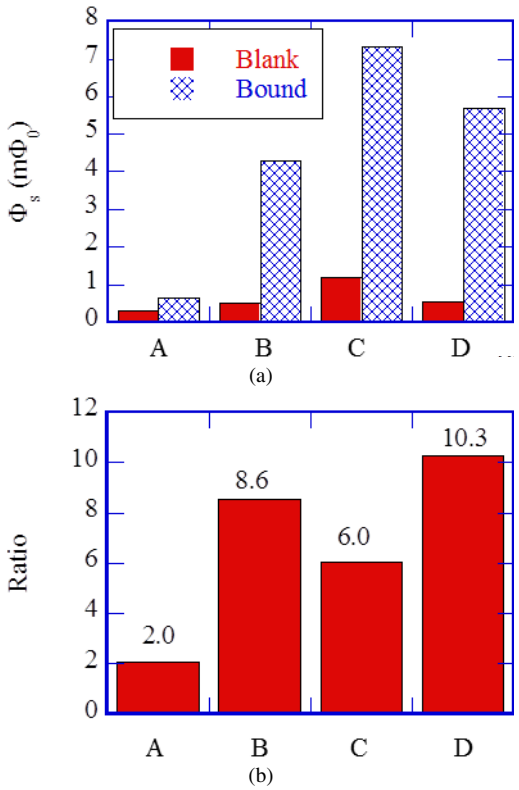

Fig. 5 (a) Bound and blank signals obtained with four different methods. Methods A to D are listed in Table 1. (b) Ratio between the bound and blank signals given in Eq. (1).

$$Ratio = \frac{\text{Bound signal } (N_B = 1.3 \times 10^5)}{\text{Blank signal } (N_B = 0)} \quad (1)$$

The ratios are 2.0 and 8.6 for cases A and B, respectively. Therefore, reaction field B_{re} is useful for increasing the detection sensitivity.

3.2 Magnetization

As shown in Fig. 3 (b), magnetic moments $\boldsymbol{m}$ of the bound markers were almost aligned when the reaction field was used. However, to completely align $\boldsymbol{m}$, additional magnetization was required. We therefore applied magnetization field B_{mag}.

In method C listed in Table 1, we applied the magnetization field of B_{mag} = 40 mT for 200 ms after the binding reaction was finished [16]. In Fig. 5 (a), the blank and bound signals obtained with this method are shown. By comparing the results with those of method B, the effect of magnetization field B_{mag} is evident. As shown in Fig. 5 (a), both the blank and bound signals in case C increased compared to those of case B. The increase of the blank signal indicates that the magnetization field B_{mag} caused agglomeration of the free markers. On the other hand, the increase of the bound signal indicates that the additional alignment of $\boldsymbol{m}$ of the bound markers was caused by B_{mag}.

In Fig. 5 (b), the ratio between the bound and blank signals given by Eq. (1) is shown. In case C, the ratio is 6.0,

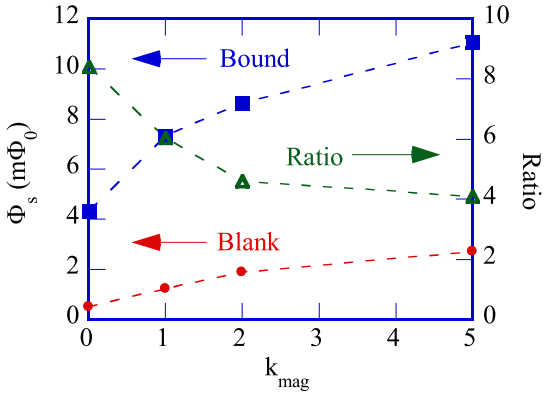

Fig. 6 Effect of the magnetization field on the blank and bound signals. The magnetization process (B_{mag} = 40 mT for 200 ms) was repeated k_{mag} times with intervals of 3 s. The ratio between the bound and blank signals is given in Eq. (1).

which is smaller than the value of 8.6 obtained for case B. This value is decreased because the rate of increase of the blank signal due to B_{mag} is larger than that of the bound signal.

To study the effect of B_{mag} on the blank and bound signals, the magnetization process (B_{mag} = 40 mT for 200 ms) was repeated k_{mag} times with intervals of 3 s. Note that we used k_{mag} = 1 in the method C shown in Fig. 5. In Fig. 6, changes of the blank and bound signals are shown when k_{mag} was increased. Both signal types increased with k_{mag}. On the other hand, the ratio given by Eq. (1) decreased with k_{mag}. Therefore, the magnetization process decreased the detection sensitivity, although the bound signal increased. Therefore, it is necessary to prevent the increase of the blank signal due to B_{mag}.

3.3 Dispersion Process

To decrease the blank signal caused by B_{mag}, we introduced a dispersion process after B_{mag} = 40 mT was applied: k_{mag} = 1 was used in the experiment. In method D listed in Table 1, the sample solution was vortex-stirred just after B_{mag} was turned off. If the binding force of the agglomerate, which was produced by B_{mag}, was weak, the agglomerate would be unraveled by the vortex stirring.

In Fig. 5 (a), the blank and bound signals obtained with method D are shown. By comparing the results with those of method C, the effect of vortex stirring is evident. As shown in Fig. 5 (a), the blank signal in case D decreased compared to case C. This result indicates that the agglomerate of the free markers was unraveled by the vortex stirring, as expected. We note that the bound signal was also decreased by the vortex stirring. This result indicates that the aggregation between the bound and free markers was also caused by field B_{mag} and that the agglomerate was unraveled by the vortex stirring.

In Fig. 5 (b), the ratio between the bound and blank signals given by Eq. (1) is shown. In method D, the ratio is 10.3. This value is the highest of the four methods.

Therefore, the dispersion process using vortex stirring is useful for highly sensitive detection of targets.

4. Field Reversal Measurement

In the practical sample, the markers that were precipitated or absorbed on the bottom of the reaction well were present, as shown in Fig. 1 (b). A blank signal was also generated by these markers. To eliminate the signal from the precipitated markers, we applied a field-reversal-measurement method [21], [22]. That is, in the measurement system shown in Fig. 1 (a), we first used a measurement field of $B_{\mathrm{mea}} = 1$ mT. Then, the polarity of the measurement field was changed to $B_{\mathrm{mea}} = -1$ mT.

Figure 7 (a) shows the signals generated from the markers when the field of $B_{\mathrm{mea}} = 1$ mT was used. There are four types of signals: Φ_{BS}, Φ_{BP}, Φ_{FS}, and Φ_{FP} were those from the bound markers in suspension, precipitated bound markers, agglomerate of free markers in suspension, and precipitated free markers, respectively. Therefore, the signal measured in this case was given by

$$\Phi(+) = \Phi_{BS}(N_B) + \mathrm{B}_{BP}(N_B) + \Phi_{FS} + \Phi_{FP}. \tag{2}$$

Note that signals Φ_{BS} and Φ_{BP}, which were generated by bound markers, increased with the number of the targets, N_{B}. On the other hand, Φ_{FS} and Φ_{FP}, which were generated by free markers, were independent of N_{B}.

When the polarity of the measurement field was changed to $B_{\mathrm{mea}} = -1$ mT, only the markers in suspension could physically rotate with the magnetic force. Therefore, signals Φ_{BS} and Φ_{FS} changed the polarity, as shown in Fig. 7 (b). On the other hand, the signal from the precipitated markers unchanged because $B_{\mathrm{mea}} = -1$ mT is much weaker than the value required for the magnetization inversion of the precipitated markers.

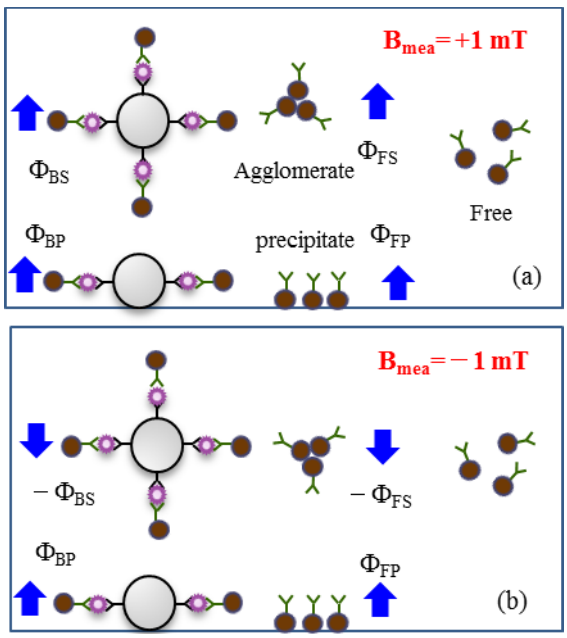

Fig. 7 Signals from the markers in the practical sample after applying (a) $\mathrm{B}_{\mathrm{mea}} = +1$ mT, and (b) $\mathrm{B}_{\mathrm{mes}} = -1$mT. The four types of signals—Φ_{BS}, Φ_{BP}, Φ_{FS}, and Φ_{FP}—were those from the bound markers in suspension, precipitated bound markers, agglomerate of free markers in suspension, and precipitated free markers, respectively.

As a result, we obtained

$$\Phi(-) = -\Phi_{BS}(N_p) + \mathrm{B}_{BP}(N_p) - \Phi_{FS} + \Phi_{FP}. \tag{3}$$

From Eqs. (2) and (3), we can obtain the following relationships:

$$\frac{\Phi(+) - \Phi(-)}{2} = \Phi_{BS}(N_B) + \Phi_{FS} \tag{4}$$

and

$$\frac{\Phi(+) + \Phi(-)}{2} = \Phi_{BP}(N_B) + \Phi_{FP}. \tag{5}$$

From Eq. (4), we can obtain the signals from the markers in suspension. On the other hand, we can obtain the signals from the precipitated markers from Eq. (5). Therefore, we can differentiate the signals between the suspended and precipitated markers.

In Fig. 8, the experimental results are shown for the cases of $B_{\mathrm{mea}} = 1$ mT and -1 mT. The samples were prepared by the method D mentioned in Sect. 3. The horizontal axis in Fig. 8 represents the number of biotin molecules, N_{B}; the vertical axis represents the detected signal. The signal $\Phi(+)$ was obtained with $B_{\mathrm{mea}} = 1$ mT, while the signal $\Phi(-)$ was obtained with $B_{\mathrm{mea}} = -1$ mT. As shown, the polarity of the signal $\Phi(-)$ was changed compared to $\Phi(+)$, as expected from Eqs. (2) and (3).

Using Eq. (4), we obtained the signal $\Phi_{\mathrm{BS}}(N_{\mathrm{B}}) + \Phi_{\mathrm{FS}}$ from the markers in suspension. The circles in Fig. 9 show the result. The signal increased with an increase in N_{B}. This behavior indicates that the increase in the signal $\Phi_{\mathrm{BS}}(N_{\mathrm{B}})$ was generated by the bound markers. On the other hand, the signal at $N_{\mathrm{B}} = 0$ represented Φ_{FS}. Note that signal Φ_{FS} was generated by the agglomerate of free markers in suspension.

Using Eq. (5), we obtained the signal $\Phi_{\mathrm{BP}}(N_{\mathrm{B}}) + \Phi_{\mathrm{FP}}$ from the precipitated markers. The squares in Fig. 9 show the result. The signal was almost constant and independent

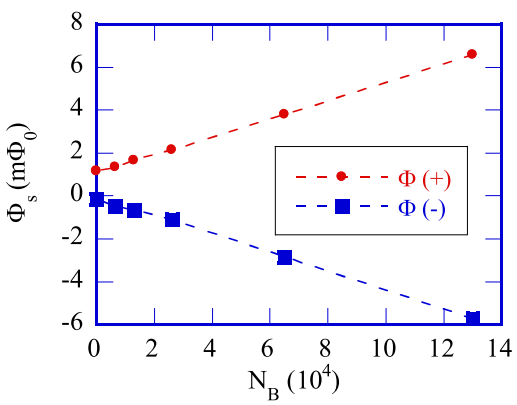

Fig. 8 Relationship between detected signal Φ_{s} and the number of biotin molecules, N_{B}. Signals $\Phi(+)$ and $\Phi(-)$ were obtained for $B_{\mathrm{mea}} = +1$ mT and -1 mT, respectively.

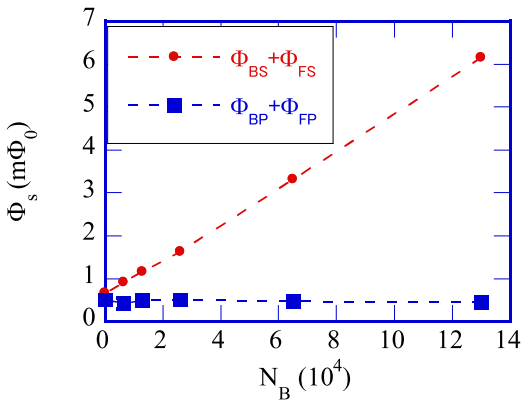

Fig. 9 Signal from suspended and precipitated markers. Signal $\Phi_{BS}(N_B) + \Phi_{FS}$ was obtained from Eq. (4) and represents the signal from markers in suspension. Signal $\Phi_{BP}(N_B) + \Phi_{FP}$ was obtained from Eq. (5) and represents the signal from the precipitated markers.

of N_B. This result indicates that $\Phi_{BP}(N_B)$ was almost zero; in other words, precipitated bound markers did not exist in this case. On the other hand, the signal at $N_B = 0$ represented Φ_{FP}. This result means that precipitated free markers existed in this case. As shown in Fig. 9, the value of Φ_{FP} was nearly the same as that of Φ_{FS} in the present case.

5. Detection Sensitivity

The relationship between $\Phi_{BS}(N_B) + \Phi_{FS}$ and N_B shown in Fig. 9 was used to detect the biotin molecules. The minimum detectable number was $N_{B,min} = 6{,}500$. Considering that the sample volume was 60 μL, this value corresponds to the molecular number concentration of 1.8×10^{-19} mol/ml. Since the typical sensitivity of the optical method called ELISA is around 5×10^{-18} mol/ml, this result indicated a high sensitivity of the present method.

6. Conclusion

In this paper, we presented improved methods for liquid-phase target detection. First, we presented a method for sample preparation and magnetization of bound markers. We introduced a reaction field, B_{re}, during the binding reaction between the markers and targets. We additionally introduced a dispersion process after magnetization of bound markers. With these methods, we could obtain a strong signal from the bound markers without increasing the blank signal of the free markers. Next, we presented a field-reversal measurement procedure that can differentiate the signal from the markers in suspension from that of the precipitated markers. Finally, we demonstrated the detection of biotin molecules using the improved detection method. The minimum detectable molecular number concentration was 1.8×10^{-19} mol/ml, which indicates the high sensitivity of the present method.

Acknowledgments

This work was partly supported by Grant-in-Aid for Scientific Research (S) 15H05764, Japan Society for the Promotion of Science.

References

[1] J. Lange, R. Kötitz, A. Haller, L. Trahms, W. Semmler, and W. Weitschies, "Magnetorelaxometry—A new binding specific detection method based on magnetic nanoparticles," J. Magn. Magn. Mater., vol.252, pp.381–383, 2002.
[2] H.L. Grossman, W.R. Myers, V.J. Vreeland, R. Bruehl, M.D. Alper, C.R. Bertozzi, and J. Clarke, "Detection of bacteria in suspension by using a superconducting quantum interference device," PNAS U. S. A., vol.101, no.1, pp.129–134, 2004.
[3] D. Eberbeck, F. Wiekhorst, U. Steinhoff, K.O. Schwarz, A. Kummrow, M. Kammel, J. Neukammer, and L. Trahms, "Specific binding of magnetic nanoparticle probes to platelets in whole blood detected by magnetorelaxometry," J. Magn. Magn. Mater., vol.321, no.10, pp.1617–1620, 2009.
[4] F. Öisjöen, J.F. Schneiderman, A.P. Astalan, A. Kalabukhov, C. Johansson, and D. Winkler, "A new approach for bioassays based on frequency- and time-domain measurements of magnetic nanoparticles," Biosens. Bioelectron., vol.25, no.5, pp.1008–1013, 2010.
[5] H.J. Hathaway, K.S. Butler, N.L. Adolphi, D.M. Lovato, R. Belfon, D. Fegan, T.C. Monson, J.E. Trujillo, T.E. Tessier, H.C. Bryant, D.L. Huber, R.S. Larson, and E.R. Flynn, "Detection of breast cancer cells using targeted magnetic nanoparticles and ultra-sensitive magnetic field sensors," Breast Cancer Res., vol.13, R108, 2011.
[6] B.T. Dalslet, C.D. Damsgaard, M. Donolato, M. Strømme, M. Strömberg, P. Svedlindh, and M. Hansen, "Bead magnetorelaxometry with an on-chip magnetoresistive sensor," Lab Chip, vol.11, no.2, pp.296–302, 2011.
[7] F. Öisjöen, J.F. Schneiderman, M. Zaborowska, K. Shunmugavel, P. Magnelind, A. Kalaboukhov, K. Petersson, A.P. Astalan, C. Johansson, and D. Winkler, "Fast and sensitive measurement of specific antigen-antibody binding reactions with magnetic nanoparticles and HTS SQUID," IEEE Trans. Appl. Supercond., vol.19, no.3, pp.848–852, 2009.
[8] K. Enpuku, Y. Tamai, T. Mitake, T. Yoshida, and M. Matsuo, "Ac susceptibility measurement of magnetic markers in suspension for liquid phase immunoassay," J. Appl. Phys., vol.108, no.3, 034701, 2010.
[9] J.J. Chieh, S.-Y. Yang, H.-E. Horng, C.Y. Yu, C.L. Lee, H.L. Wu, C.-Y. Hong, and H.-C. Yang, "Immunomagnetic reduction assay using high-T_c superconducting-quantum-interference-device-based magnetosusceptometry," J. Appl. Phys., vol.107, no.7, 074903, 2010.
[10] M.J. Chiu, H.E. Horng, J.J. Chien, S.H. Liao, C.H. Chen, B.Y. Shih, C.C. Yang, C.L. Lee, T.F. Chen, S.Y. Yang, C.Y. Hong, and H.C. Yang, "Multi-channel SQUID-based ultra-high-sensitivity in-vitro detections for bio-markers of Alzheimer's disease via immuno-magnetic reduction," IEEE Trans. Appl. Supercond., vol.21, no.3, pp.477–480, 2011.
[11] R.S. Gaster, L. Xu, S.-J. Han, R.J. Wilson, D.A. Hall, S.J. Osterfeld, H. Yu, and S.X. Wang, "Quantification of protein interactions and solution transport using high-density GMR sensor arrays," Nature Nanotech., vol.6, no.5, pp.314–320, 2011.
[12] A. Shoshi, J. Schotter, P. Schroeder, M. Milnera, P. Ertl, V. Charwat, M. Purtscher, R. Heer, M. Eggeling, G. Reiss, and H. Brueckl, "Magnetoresistive-based real-time cell phagocytosis monitoring," Biosens. Bioelectron., vol.36, no.1, pp.116–122, 2012.
[13] X. Zhang, D.B. Reeves, I.M. Perreard, W.C. Kett, K.E. Griswold, B.

Gimi, and J.B. Weaver, "Molecular sensing with magnetic nanoparticles using magnetic spectroscopy of nanoparticle Brownian motion," Biosens. Bioelectron., vol.50, pp.441–446, 2013.
[14] K. Enpuku, H. Tokumitsu, Y. Sugimoto, H. Kuma, N. Hamasaki, A. Tsukamoto, T. Mizoguchi, A. Kandori, K. Yoshinaga, H. Kanzaki, and N. Usuki, "Fast detection of biological targets with magnetic marker and SQUID," IEEE Trans. Appl. Supercond., vol.19, no.3, pp.844–847, 2009.
[15] H. Kuma, H. Oyamada, A. Tsukamoto, T. Mizoguchi, A. Kandori, Y. Sugiura, K. Yoshinaga, K. Enpuku, and N. Hamasaki, "Liquid phase immunoassays utilizing magnetic markers and SQUID magnetometer," Clin. Chem. Lab. Med., vol.48, no.9, pp.1263–1269, 2010.
[16] S. Uchida, Y. Higuchi, Y. Ueoka, T. Yoshida, K. Enpuku, S. Adachi, K. Tanabe, A. Tsukamoto, and A. Kandori, "Highly sensitive liquid-phase detection of biological targets with magnetic markers and high Tc SQUID," IEEE Trans. Appl. Supercond., vol.24, no.4, 1600105, 2014.
[17] A. Tsukamoto, S. Adachi, Y. Oshikubo, and K. Tanabe, "Design and fabrication of directly-coupled HTS-SQUID magnetometer with a multi-turn input coil," IEEE Trans. Appl. Supercond., vol.23, no.3, 6353540, 2013.
[18] K. Enpuku, Y. Ueoka, T. Sakakibara, M. Ura, T. Yoshida, T. Mizoguchi, and A. Kandori, "Liquid-phase immunoassay utilizing binding reactions between magnetic markers and targets in the presence of a magnetic field," Appl. Phys. Express, vol.7, no.9, 097001, 2014.
[19] T. Sasayama, T. Yoshida, M.M. Saari, and K. Enpuku, "Comparison of volume distribution of magnetic nanoparticles obtained from M-H curve with a mixture of log-normal distributions," J. Appl. Phys., vol.117, no.17, 17D155, 2015.
[20] Y. Higuchi, S. Uchida, A.K. Bhuiya, T. Yoshida, and K. Enpuku, "Characterization of magnetic markers for liquid-phase detection of biological targets," IEEE Trans. Magn., vol.49, no.7, pp.3456–3459, 2013.
[21] A. Tsukamoto, T. Mizoguchi, A. Kandori, H. Kuma, N. Hamasaki, H. Kanzaki, N. Usuki, K. Yoshinaga, and K. Enpuku, "Development of a SQUID system using field reversal for rapidly detecting bacteria," IEEE Trans. Appl. Supercond., vol.19, no.3, pp.853–856, 2009.
[22] M. Ura, Y. Ueoka, K. Nakamura, T. Sasayama, T. Yoshida, and K. Enpuku, "New Detection Method of Biological Targets Based on HTS SQUID and Magnetic Marker," IEEE ISEC 2015 proceeding (in press).

Masakazu Ura received the B. Eng. and M. Eng. degrees from Kyushu University in 2014 and 2016, respectively. During the master course in Kyushu University, he engaged in the development of SQUID system for biological immunoassay.

Kohei Noguchi received the B. Eng. and M. Eng. degrees from Kyushu University in 2014 and 2016, respectively. During the master course in Kyushu University, he developed the liquid-phase detection technique utilizing Brownian relaxation of magnetic nanoparticles.

Yuta Ueoka received the B. Eng. and M. Eng. degrees from Kyushu University in 2013 and 2015, respectively. During the master course in Kyushu University, he engaged in the development of SQUID system for biological immunoassay.

Kota Nakamura received the B. Eng. degrees from Kyushu University in 2015, and is now master course student of Graduate School of Information Science and Electrical Engineering, Kyushu University. He has been developing a high-sensitive detection method of biological targets based on high T_c SQUID magnetometer.

Teruyoshi Sasayama received the B. Eng., M. Eng., and Dr. Eng. degrees from Kyoto University in 2007, 2009, and 2012, respectively. He is an Assistant Professor in the Faculty of Information Science and Electrical Engineering, Kyushu University. He has been engaged in analysis of magnetic nanoparticle properties. His current interest is the development of the algorithm for magnetic particle imaging.

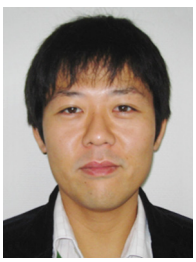

Takashi Yoshida received the B. Eng., M. Eng., and Dr. Eng. degrees from Kyushu University in 1998, 2000 and 2003, respectively. He is an Associate Professor in the Faculty of Information Science and Electrical Engineering, Kyushu University. He has been engaged in the biomedical applications of magnetic nanoparticles. His current interest is the development of a magnetic particle imaging system.

Keiji Enpuku received the B. Eng., M. Eng., and Dr. Eng. degrees from Kyushu University in 1976, 1978 and 1981, respectively. He is a Professor in the Research Institute of Superconductor Science and Systems, Kyushu University. He has been engaged in the superconducting electronics. His current interest is the development of high performance high T_c SQUID magnetometer and its applications.